NUMERICAL STUDY OF FLOW INHOMOGENEITY AND HEAT TRANSFER ENHANCEMENT IN STRUCTURED PACKED BEDS

by

Jingyu WANG[a,b], Jian YANG[a,b], Bengt SUNDEN[b], and Qiuwang WANG[a*]

[a]Key Laboratory of Thermo-Fluid Science and Engineering, Ministry of Education,
School of Energy and Power Engineering, Xi'an Jiaotong University, Xi'an, Shaanxi, China
[b]Division of Heat Transfer, Department of Energy Sciences, Lund University, Skåne, Sweden

Original scientific paper
https://doi.org/10.2298/TSCI200323274W

Packed beds are widely used in engineering applications due to their high specific surface area and good heat transfer characteristics. A grille-sphere composite packed bed is proposed previously and has been proved to have higher overall heat transfer coefficient than the simple cubic packing structure. In the present paper, the flow inhomogeneities in both the grille-sphere composite packed bed and the simple cubic packing are studied and the relationship between the flow inhomogeneity and the heat transfer characteristics is revealed by numerical simulations. The simulations are performed on ANSYS FLUENT software. The turbulence flow is modelled by the renormalization group k-ε model. Both dispersion of the velocity distribution and the residence time distribution are employed to assess the flow maldistribution. When the inlet velocity equals 2.17 m/s, the variance of the residence time distribution of the composite packed bed is 5.91% smaller than that of the simple cubic packing while the Nusselt number is 10.64% higher. The results indicate that less flow maldistribution can lead to heat transfer enhancement.

Keywords: *grille sphere composite packing, structured packed bed, flow inhomogeneity index, residence time distribution, flow maldistribution*

Introduction

Packed beds are widely used in a variety of industries, such as high temperature gas cooled reactors [1], energy storage systems [2] and catalytic packed bed reactors [3]. Due to the complexity of pore structure, the flow inhomogeneity in packed beds is significant and the flow will further influence the heat and mass transfer characteristics. The CFD has become a powerful tool to study the fluid flow in packed beds and the particle-resolved simulation can provide the most rigorous description of packed beds [4]. For example, Wu *et al*. [5] employed the discrete element method combined with CFD (DEM-CFD) simulation to investigate the helium flow characteristics in randomly packed beds at rather low Reynolds numbers and they studied the relationship between the local velocity and the pore structure. The similar numerical method was used by Zhang *et al*. [6] and their results showed that the local pack-

*Corresponding author, e-mail: wangqw@mail.xjtu.edu.cn

ing-structure parameters have significant effects not only on the local velocity and pressure fields but also on macroscopic quantities, such as the average pressure gradient along the flow direction of the packed bed. Dixon [7] studied the local transport and reaction rates in a fixed bed reactor with methane steam reforming reaction by the particle-resolved simulation. Dong *et al*. [8] carried out the particle-resolved CFD simulations to have insights of the temperature profiles in fixed bed reactors.

Research has shown that the flow inhomogeneity in packed beds can have a significant influence on macroscopic parameters, such as the pressure drop, heat transfer and mass transfer performances. The study of the flow inhomogeneity is therefore important. The investigations of the flow inhomogeneity mainly contain two methods, one is the direct way and the other is the indirect way.

In the direct way, the dispersion of velocity on the cross-sections along the flow direction is evaluated. In this area, Petrova *et al*. [9] reviewed the estimation methods of gas-flow maldistributions in packed beds and recommended the equations to calculate the maldistribution factor. Marek [10] studied the flow maldistributions in packed beds with different particle shapes and inlet configurations by calculating the velocity deviation. In the indirect way, residence time distribution (RTD) is a useful method to assess the flow maldistribution. This method is based on the study of transient state. After obtaining the steady flow field, a non-diffusive tracer was injected into the packed bed and the tracer concentration on the outlet was monitored. The flow inhomogeneities were evaluated by the RTD curve. For instance, Atmakidis and Kenig [11] studied the RTD in packed beds with small tube-to-particle ratios to assess the influence of wall effect. Pawlowski *et al*. [12] studied RTD in monolithic porous columns reconstructed from X-ray tomography data and compared it with the experimental results. The RTD in multi-orifice baffled tubes was numerically studied where the concentration-time profile of the tracer was analysed [13]. Guo *et al*. [14] revealed that there is a relationship between the velocity distribution on a cross-section and the RTD curve. Wang *et al*. [15] studied the RTD in three typical structured packed bed and reported a relationship between the RTD and the heat transfer. Stepanov *et al*. [16] studied the residence time by Lagrange particle tracking method in CFD to determine the influence of baffles in a combustion chamber. Tomanović *et al*. [17] studied the gas desulfurization process also by Lagrange particle tracking method and found that the distribution, dispersion and residence time of sorbent particles in the furnace have a considerable influence on the desulfurization process.

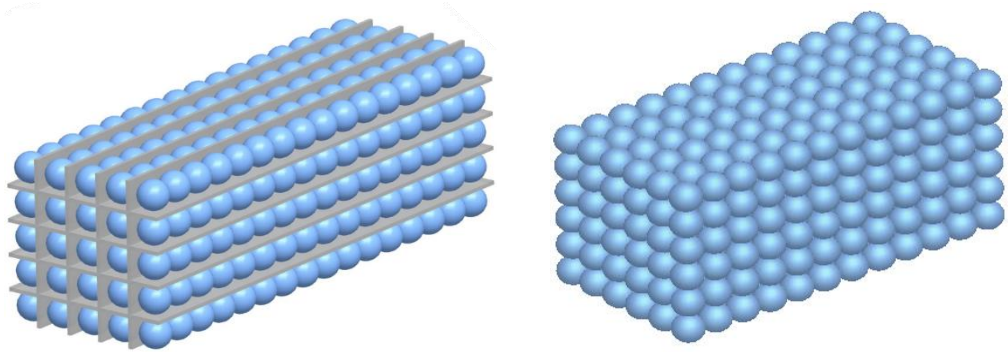

(a) (b)

Figure 1. Diagrams of GSCPB (a) and SC (b) packing

From aforementioned, it can be seen that the flow maldistribution is closely related to the heat/mass transfer. Better flow homogeneity can lead to stronger heat transfer performance. In our previous study [18], we designed a grille-sphere composite packed bed (GSCPB) and studied the particle-to-fluid heat transfer characteristics by experiments. Besides, the Nusselt number in GSCPB is compared to that of a simple cubic (SC) packed bed with the same particle diameter since these two structures are almost the same expect for the grille wall, as shown in fig. 1. The experimental results showed that the Nusselt number in GSCPB is higher than the SC packing structure. As a continuation of the previous study, the present paper will study the flow inhomogeneity in these two packing structures and try to reveal the relationship between the flow inhomogeneity and the heat transfer. The flow inhomogeneity is investigated by both the direct way and the indirect way. The study is carried out by ANSYS FLUENT 17.0.

Model description

From fig. 1(a), it can be seen that, in GSCPB, the whole flow channel is divided into several parallel sub-channels and each sub-channel behaves the same theoretically. Therefore, only one channel is chosen in the numerical study so as to reduce the computational time. Here, the grille wall is considered to be adiabatic and the thickness of the grille wall is neglected. Besides, only ten particles are stacked since ten particles can guarantee the fully developed flow [19]. The diameter of the particle is 12 mm, which is the same as the experiment [18]. The simplified geometry of GSCPB is shown in fig. 2, where a clear inlet section and an outlet section are added to make the velocity uniform and to avoid backflow. The lengths of the inlet section and the outlet section are 30 mm and 80 mm, respectively.

As for SC packing shown in fig. 1(b), the geometry is periodic and thus one channel can represent the whole structure [20]. Again, ten particles are used in the simulation. The simplified computational model is the same with GSCPB except for the boundary conditions of the walls around, which are symmetric boundaries in SC packing.

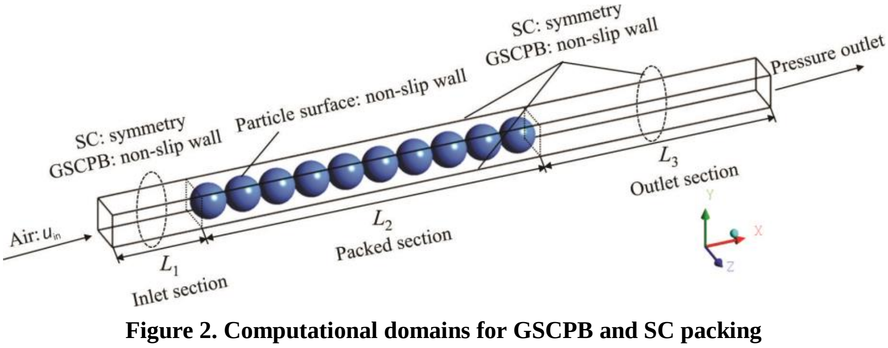

Figure 2. Computational domains for GSCPB and SC packing

Numerical method

In the present work, the continuity equation, 3-D Navier-Stokes equations and energy equation are employed for the simulations. The finite volume analysis software ANSYS FLUENT 17.0 is used to solve the equations. The studied Reynolds number, $Re_h = \rho_f(u_{in}/\varphi)d_h/\mu$, in two structures are both larger than 300, where the flow would be turbulent flow inside [21]. The renormalization group (RNG) k-ε model and the scalable wall-function treatment with $y^+ > 11.225$ (dimensionless distance of the wall grid elements) are adopted for the simulation. The RNG k-ε turbulence model is applicable to the small-scale eddies, which are independent of the larger-scale phenomena that create them, and it is more suitable for modelling turbulent flow in packed beds [22].

The conservation equations for mass, momentum, and energy are:

$$\nabla\left(\rho_{\mathrm{f}}\vec{\mathrm{v}}\right)=0 \tag{1}$$

$$\nabla\left(\rho_{\mathrm{f}}\vec{\mathrm{v}}\vec{\mathrm{v}}\right)=-\nabla p+\nabla\mu_{\mathrm{eff}}\left[\nabla\vec{\mathrm{v}}+\left(\nabla\vec{\mathrm{v}}\right)^{T}\right] \tag{2}$$

$$\nabla\left(\rho_{\mathrm{f}}\vec{\mathrm{v}}T_{\mathrm{f}}\right)=\nabla\left[\alpha c_{p}\mu_{\mathrm{eff}}\nabla T_{\mathrm{f}}\right] \tag{3}$$

The transport equations for RNG k-ε model are:

$$\begin{cases} k:\ \rho_{\mathrm{f}}\left(\vec{\mathrm{v}}\nabla k\right)=\nabla\cdot\left[\alpha_{k}\mu_{\mathrm{eff}}\nabla k\right]+P_{\mathrm{k}}-\rho_{\mathrm{f}}\varepsilon \\ \varepsilon:\ \rho_{\mathrm{f}}\left(\vec{\mathrm{v}}\nabla\varepsilon\right)=\nabla\cdot\left[\alpha_{\varepsilon}\mu_{\mathrm{eff}}\nabla\varepsilon\right]+\dfrac{c_{\varepsilon1}\varepsilon}{k}P_{\mathrm{k}}-c_{\varepsilon2}\rho_{\mathrm{f}}\dfrac{\varepsilon^{2}}{k} \end{cases} \tag{4}$$

The details of the equations can be found in the Theory Guide of ANSYS FLUENT [23].

In the simulations, the inlet velocity and temperature of air are fixed (u_{in} = 2.17 m/s, T_{in} = 300 K). The outlet flow and heat transfer of air are fully developed. All particle surfaces are set to non-slip wall boundary conditions. The 7$^{\mathrm{th}}$ particle is supposed to have a constant temperature of 333 K while others are adiabatic. By doing so, the heat transfer characteristics in the fully developed region can be obtained. In GSCPB, the surrounded walls are set to non-slip wall boundary conditions while in SC packing, the surrounded walls are set as symmetric boundary conditions.

The SIMPLE algorithm is employed to couple the velocities and pressure. The second-order upwind scheme is selected for the convective terms in the momentum, energy and turbulence equations. The residual of the calculation is less than 10^{-6} to guarantee convergence of the steady state.

After the fluid-flow of the steady-state is obtained, the species transport equation at the transient state is activated to calculate the RTD. In order to imitate a Dirac pulse, the tracer concentration of the inlet is set to unity at the first-time step and then reduced to zero at the following time step. The tracer concentration of the fluid domain is calculated and followed until it completely exits the outlet. The duration time of the tracer injection should be lower than 1% of the whole mean residence time [15]. The time step used in the present study is 5×10^{-5} s. The convergence of each time step is reached when the residual of the tracer concentration is less than 10^{-6} and the total time step of the calculation is 10000. From the tracer concentration averaged over the cross section, C_{ave}, the RTD function can be calculated [11]:

$$E\left(t\right)=\frac{C_{\mathrm{ave}}\left(t\right)}{\int_{0}^{\infty}C_{\mathrm{ave}}\left(t\right)dt} \tag{5}$$

The mean residence time (MRT), τ, and the variance of the residence time distribution (VRTD), σ_{t}, can be calculated by the eqs. (6) and (7). Here, VRTD is used to quantify the flow maldistribution in the packed bed where smaller value corresponds to better velocity uniformity at the cross-sections [11]:

$$\tau=\frac{\int_{0}^{\infty}tC_{\mathrm{ave}}\left(t\right)\mathrm{d}t}{\int_{0}^{\infty}C_{\mathrm{ave}}\left(t\right)\mathrm{d}t} \tag{6}$$

$$\sigma_t = \frac{\int_0^\infty (t-\tau)^2 C_{\text{ave}}(t)\,\mathrm{d}t}{\int_0^\infty C_{\text{ave}}(t)\,\mathrm{d}t} = \frac{\int_0^\infty t^2 C_{\text{ave}}(t)\,\mathrm{d}t}{\int_0^\infty C_{\text{ave}}(t)\,\mathrm{d}t} - \tau^2 \tag{7}$$

All computations are launched on a workstation with Intel® Xeon™ E5-2695 v4 CPU and 128 GB RAM. The computational time is around six hours for the steady-state and about 72 hours for the transient state when 20 cores are used. In the grid generation process, unstructured tetrahedral mesh is applied. All particles are shrunk to 99% of the original size to avoid the low mesh quality at the contact points. The grid independence test and model validation test can be found in our previous study [18] and will not be repeated here.

Results and discussion

In this section, the flow field in the steady-state and the RTD in the transient state are analysed to evaluate the flow inhomogeneity in both structures. The heat transfer characteristics are also introduced.

Flow field

The streamline in the SC packing is displayed in fig. 3. A higher velocity can be found at the corners of the square channel whereas backflow appears between particles. The streamline in GSCPB has a similar feature which is not shown here. The flow maldistribution is obvious in packed beds.

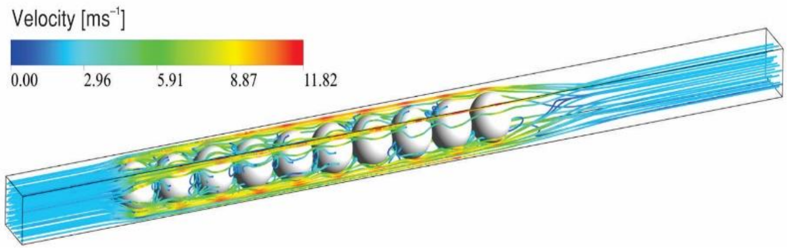

Figure 3. Streamline in the SC packing

In order to quantitatively analyse the flow maldistribution inside the packed bed, the average velocity and the standard deviation of the velocity on the cross-sections are calculated. Here, the velocity refers to the streamwise component (X-velocity, u_x). Marek [10] has pointed out that using the streamwise component instead of flow velocity magnitude makes it more sensitive to flow non-uniformity. A series of cross-sections along the flow direction is used for the analysis. The 20 equally spaced sections in one particle cell are created and there are totally 201 sections in the packed section. The standard deviation of the velocity in each cross-section, std(u_x), is calculated by:

$$\text{std}(u_x) = \sqrt{\frac{\sum_{i=1}^{n} A_i \left(u_x - u_{x,\text{ave}}\right)^2}{\sum_{i=1}^{n} A_i}}, \quad u_{x,\text{ave}} = \frac{\sum_{i=1}^{n} u_x A_i}{\sum_{i=1}^{n} A_i} \tag{8}$$

where n is the cell number of a certain cross section and A_i is the area of the cell.

The obtained average X-velocity, $u_{x,\text{ave}}$, and standard deviation of X-velocity, std(u_x), of the cross-sections along the flow direction are shown in fig. 4. It can be seen that the X-velocities averaged over the cross-sections in GSCPB and SC packing are the same because the average velocity in the cross-section is only dependent on the flow area, which has the same value in both configurations. However, the variations of the standard deviation of the X-velocity along the axial direction are not the same. From the variations of the standard deviation, the entrance effect can be found in the first three layers and from that on, the standard deviation of velocity shows a periodic trend, which indicates the fully developed flow. In the fully developed region, the std(u_x) in GSCPB is smaller than that of SC packing, especially in the windward side.

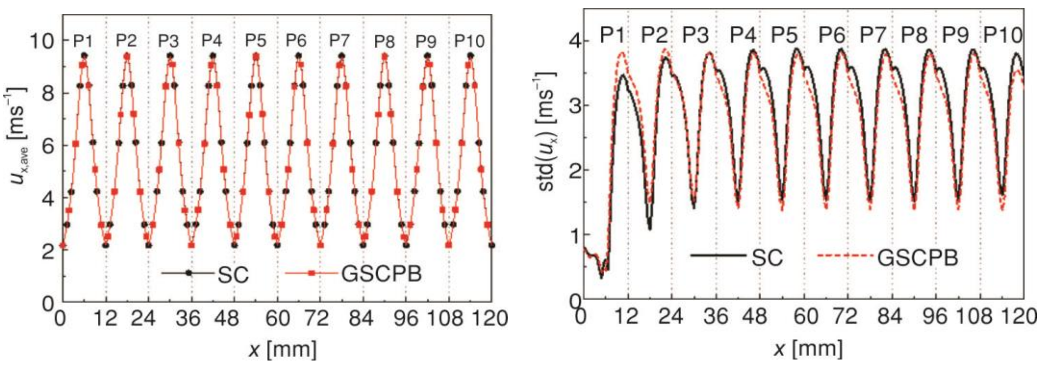

(a) **(b)**

Figure 4. Average X-velocity (a) and standard deviation of X-velocity (b) of cross-sections along the axial direction in GSCPB and SC packing

In the present paper, the flow inhomogeneity index, I, is introduced, which has the following expression:

$$I = \frac{\dfrac{\sum_{j=1}^{m} \text{std}(u_x)}{m}}{u_{\text{in}}} \tag{9}$$

where m is the number of the cross-sections.

The flow inhomogeneity indexes in the fully developed region of GSCPB and SC packing are 1.34 and 1.42, respectively. This indicates that the velocity field in GSCPB is more uniform.

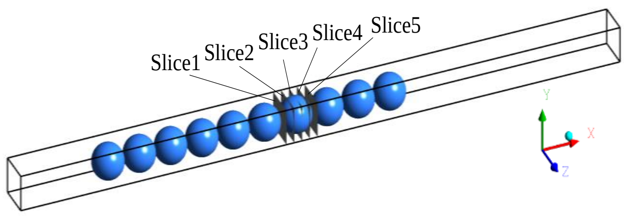

Figure 5. Positions of five slices in GSCPB and SC packing

For a clear look of the flow maldistribution, X-velocity contours of several typical cross sections are shown. Figure 5 demonstrates the position of the cross-sections and fig. 6 shows the X-velocity contours in both structures where S denotes Slice for short. The velocity distribution of

Slice 5(S5) is not shown since it is the same as Slice 1(S1). A much more uniform velocity field can be found in GSCPB, especially through S3.

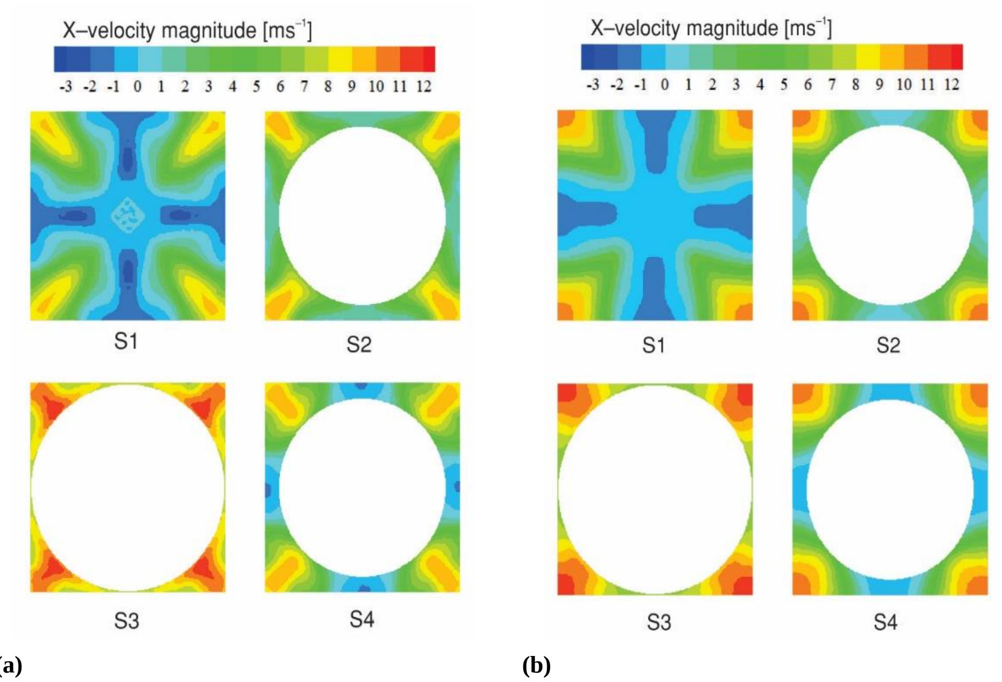

Figure 6. X-velocity distributions in four slices in GSCPB (a) and SC (b) packing

Residence time distribution analysis

The RTD curves of Slices 1-5 in both structures are shown in fig. 7. In general, since the RTD curve is a reflection of the cumulative flow inhomogeneity of whole flow passage, the RTD curve of cross-sections should be wider and lower as the flow advances. This can be found from S1 and S5. Although S1 and S5 in one structure has the same velocity distributions, the RTD curve of S5 is lower and wider than that of S1.

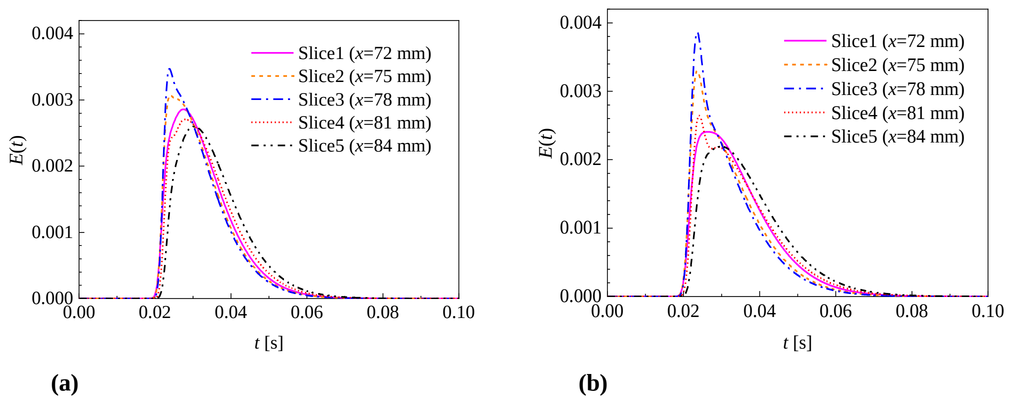

Figure 7. The RTD curves in GSCPB (a) and SC (b) packing

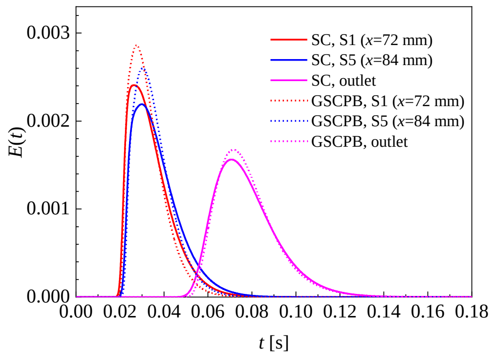

Figure 8. Comparison of RTD curves in GSCPB and SC packing

Table 1. The VRTD in GSCPB and SC packing [s^2]

	S1 (x = 72 mm)	S5 (x = 84 mm)	Outlet
GSCPB	$6.55\cdot10^{-5}$	$7.50\cdot10^{-5}$	$1.91\cdot10^{-4}$
SC	$9.53\cdot10^{-5}$	$1.10\cdot10^{-4}$	$2.03\cdot10^{-4}$

On the other hand, the RTD curve is related to the flow inhomogeneity of that slice, where higher and thinner curve is supposed to have more uniform velocity distribution, therefore, it can be learned that S3 has the most uniform velocity distribution in both structures. This can be verified by the velocity contours shown in fig. 6.

To compare the flow maldistribution in the two structures, the RTD curves of the same position are used. Here, S1, S5 and the outlet are chosen, as shown in fig. 8. It can be seen that at the same position, the RTD curve of GSCPB is a little higher and thinner than that of SC packing, indicating that the flow inhomogeneity is more significant in SC packing. The VRTD of the selected slices in both structures are listed in tab. 1. From here, one can know that the VRTD is becoming larger when the flow advances, indicating that the flow maldistribution is getting more obvious. Besides, for S1, S5 and the outlet, the VRTD decreased by 31.27%, 31.82%, and 5.91%, respectively, in GSCPB compared with SC packing. The results prove that the flow maldistribution is less bad in GSCPB. The results obtained here coincide with the flow inhomogeneity index.

Heat transfer

The wall heat flux distributions on the *active* sphere (7$^{\text{th}}$) surface in both structures are displayed in fig. 9. From the figure, similar wall heat flux distributions can be found in both structures where high heat flux appears at the windward side and low heat flux occurs at the leeward side. The maximum wall heat flux in GSCPB is 6009 W/m^2 while the maximum value in SC packing is 5343 W/m^2. Besides, the region with high values covers a larger percentage of the surface area in GSCPB than that in SC packing. From the results, one can know that the heat transfer between the particle and the fluid is stronger in GSCPB. The particle-to-fluid Nusselt number, $\text{Nu}_{\text{sf}} = qd_p/[(T_w - T_f)\lambda]$, in GSCPB and SC are 49.93 and 45.13, respectively, where the Nusselt number in GSCPB is 10.64% higher.

From the velocity and heat transfer results, one can find that better flow uniformity leads to stronger heat transfer when the pore structures are the same. This can be helpful for structural design of packed bed.

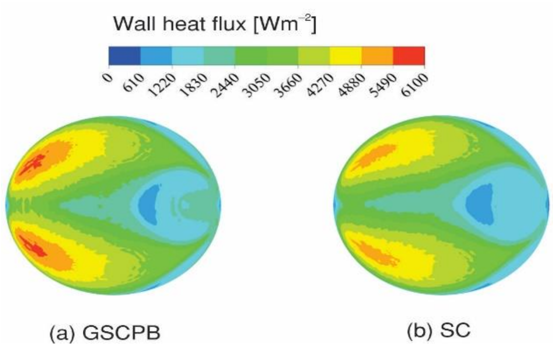

(a) **(b)**

Figure 9. Comparison of wall heat flux in GSCPB (a) and SC (b) packing

Conclusions

In the present paper, the flow maldistribution and heat transfer in the GSCPB and SC packing were numerically studied. The velocity distributions of the steady-state and the RTD of the transient state were analysed to evaluate the flow maldistribution. The main conclusions are as follows.

- The flow inhomogeneity index, which is introduced in the present paper, is 1.34 for GSCPB and 1.42 for SC packing. The results reveal that the velocity distribution is more uniform in GSCPB.
- The VRTD of the outlet in GSCPB is 5.91% smaller than that of SC packing under the same inlet velocity, which proves that the flow inhomogeneity in SC packing is more serious.
- The particle-to-fluid Nusselt number of GSCPB is 10.64% higher than that of the SC packing under the same inlet velocity, which indicates that the reduction of flow inhomogeneity can lead to heat transfer enhancement when the pore structures are the same.

Acknowledgment

This work is financially supported by the National Key Research and Development Program of China (No. 2017YFB0603500) and the National Natural Science Foundation of China (No. 51536007). The first author acknowledges the financial support (No. 201806280098) from China Scholarship Council (CSC) for her one-year visit to Lund University.

Nomenclature

A – area [m^2]
c_p – specific heat capacity at constant pressure [Jkg^{-1}K^{-1}]
$c_{\varepsilon 1}, c_{\varepsilon 2}$ – turbulence model constants in ε equation [–]
C – mass fraction of tracer [−]
d – diameter [m]
E – RTD function [–]
I – flow inhomogeneity index [−]
k – turbulent kinetic energy [m^{2}s^{-2}]
m – number of cross-sections [−]
n – cell number [−]
Nu – Nusselt number [−]
p – pressure [Pa]
P_k – shear production of turbulence [kgm^{-1}s^{-3}]
q – heat flux [Wm^{-2}]
Re – Reynolds number [−]
T – temperature [K]
t – time [s]
u – velocity [ms^{-1}]
$\vec{\mathrm{v}}$ – velocity vector [ms^{-1}]
x – x-coordinate [m]
y^+ – dimensionless distance of the wall grid elements [−]

Greek symbols

α – inverse effective Prandtl number [–]
ε – turbulent dissipation rate [m^{2}s^{-3}]
λ – heat conductivity [Wm^{-1}K^{-1}]
μ – dynamic viscosity [kgm^{-1}s^{-1}]
ρ – density [kgm^{-3}]
σ_t – variance of residence time distribution [s^2]
τ – mean residence time [s]
φ – porosity [−]

Subscripts

ave – average
eff – effective
f – fluid
h – hydraulic
i – i$^{\mathrm{th}}$ cell
in – inlet
p – particle
sf – particle-to-fluid
w – wall
x – X direction

References

[1] du Toit, C.G., van Antwerpen, H.J., Effect of Reactor Vessel Cooling Insulation and Reflector Heat Pipes on the Temperatures of a Pebble-Bed Reactor Using a System CFD Approach, *Nucl. Eng. Des.*, *357* (2020), pp. 110-421

[2] Li X, *et al.*, Investigation of the Dynamic Characteristics of a Thermal Energy Storage Unit Filled with Multiple Phase Change Materials, *Thermal Science*, *22* (2018), Suppl. 2, pp. S527-S533
[3] Yun, J., Yu, S., Transient Behavior of 5 kw Class Shell-and-Tube Methane Steam Reformer with Intermediate Temperature Heat Source, *Int. J. Heat Mass Transf.*, *134* (2019), pp. 600-609
[4] Wehinger, G.D., *et al.*, Modeling Pore Processes for Particle-Resolved CFD Simulations of Catalytic Fixed-Bed Reactors, *Comput Chem Eng*, *101* (2017), pp. 11-22
[5] Wu, Z., *et al.*, DEM-CFD Simulation of Helium Flow Characteristics in Randomly Packed Bed for Fusion Reactors, *Prog. Nucl. Energy*, *109* (2018), pp. 29-37
[6] Zhang, J., *et al.*, Computational Fluid Dynamics Flow Simulations in Discrete Element Method-Resolved Packed Beds, *J Fluids Eng*, *141* (2019), 3, pp. 31-304
[7] Dixon, A.G., Local Transport and Reaction Rates in a Fixed Bed Reactor Tube: Endothermic Steam Methane Reforming, *Chem. Eng. Sci.*, *168* (2017), pp. 156-177
[8] Dong, Y., *et al.*, What Happens in a Catalytic Fixed-Bed Reactor for n-Butane Oxidation to Maleic Anhydride? Insights From Spatial Profile Measurements and Particle Resolved CFD Simulations, *Chem. Eng. J.*, *350* (2018), pp. 799-811
[9] Petrova, T., *et al.*, Estimations of Gas Flow Maldistribution in Packed-Bed Columns, *Chem Eng Technol*, *31* (2008), 12, pp. 1723-1729
[10] Marek, M., Gas Flow Maldistribution in Random Packed Beds of Non-Spherical Particles–a CFD Study, *Chem. Eng. Sci.*, *197* (2019), pp. 296-305
[11] Atmakidis, T., Kenig, E.Y., Numerical Analysis of Residence Time Distribution in Packed Bed Reactors with Irregular Particle Arrangements, *Chem. Prod. Process. Model.*, *10* (2015), 1, pp. 17-26
[12] Pawlowski, S., *et al.* CFD Modelling of Flow Patterns, Tortuosity and Residence Time Distribution in Monolithic Porous Columns Reconstructed from X-ray Tomography Data, *Chem. Eng. J.*, *350* (2018), pp. 757-766
[13] González-Juárez, D., *et al.*, Residence Time Distribution in Multiorifice Baffled Tubes: A numerical Study, *Chem Eng Res Des*, *118* (2017), pp. 259-269
[14] Guo, B.Y., *et al.*, Simulation of Turbulent Flow in a Packed Bed, *Chem Eng Technol*, *29* (2006), 5, pp. 596-603
[15] Wang, J., *et al.*, Assessment of Flow Pattern and Temperature Profiles by Residence Time Distribution in Typical Structured Packed Beds, *Numerical Heat Transfer, Part A: Applications*, *77* (2020), 6, pp. 559-578
[16] Stepanov. B.L., *et al.*, Scandinavian Baffle Boiler Design Revisited, *Therm. Sci.*, *19* (2015), 1, pp. 305-316
[17] Tomanovic, I.D., *et al.*, Numerical Tracking of Sorbent Particles and Distribution During Gas Desulfurization in Pulverized Coal-Fired Furnace, *Therm. Sci.*, *21* (2017), pp. S759-S769
[18] Wang, J.Y., *et al.*, Experimental and Numerical Study on Pressure Drop and Heat Transfer Performance of Grille-Sphere Composite Structured Packed Bed, *Appl. Energy*, *227* (2018), pp. 719-730
[19] Romkes, S., *et al.*, CFD Modelling and Experimental Validation of Particle-to-Fluid Mass and Heat Transfer in a Packed Bed at Very Low Channel to Particle Diameter Ratio, *Chem. Eng. J.*, *96* (2003), 1, pp. 3-13
[20] Yang, J., *et al.*, Computational Study of Forced Convective Heat Transfer in Structured Packed Beds with Spherical or Ellipsoidal Particles, *Chem. Eng. Sci.*, *65* (2010), 2, pp. 726-738
[21] Bu, S., *et al.*, Experimental Study of Mass Transfer and Flow Transition in Simple Cubic Packings with the Electrochemical Technique, *Electrochim. Acta*, *177* (2015), pp. 370-376
[22] Yakhot, V., Orszag, S.A., Renormalization Group Analysis of Turbulence I. Basic theory, *J Sci Comput*, *1* (1986), 1, pp. 3-51
[23] ***, ANSYS FLUENT 14.5, Theory Guide, ANSYS, Inc., Canonsburg, Penn., USA, 2012

Paper submitted: March 23, 2020
Paper revised: April 2, 2020
Paper accepted: Maz 1, 2020